KFUPM
Journal of Undergraduate Research International

Diamond Open Access 99

Article Geosciences

Surface Wave Inversion and Seismic Refraction Analysis for Near-surface Characterization in Khamis Mushait, Southwestern Saudi Arabia

Yazeed M. Alqahtani and Sherif M. Hanafy*

Cite https://doi.org/10.64589/juri/231558

Submitted: April 25, 2026 **Revised:** May 15, 2026 **Accepted:** May 17, 2026

ABSTRACT

Surface Wave Inversion (SWI) provides direct access to the most relevant parameters for assessing rigidity, weathering contrasts, and near-surface mechanical variation. However, an integrated SWI and seismic refraction workflow has not been applied to characterize the near-surface Vs structure of the southwestern Arabian Shield—a geologically complex crystalline basement terrain. Therefore, we applied SWI to seismic data acquired in the Khamis Mushait area of southwestern Saudi Arabia to estimate the near-surface velocity (Vs) structure. Seismic data acquired from a refraction survey were processed using winMASW to extract dispersion curves and perform shot-wise one-dimensional (1D) inversion. The resulting shear-wave Vs profiles were spatially integrated using Surfer to generate a pseudo-two-dimensional Vs section. The results revealed a clear increase in Vs with depth, identifying three main zones: a low-velocity near-surface layer with Vs values below 800 m/s extending to a depth of approximately 80–120 m; an intermediate transition zone with Vs ranging from approximately 800–1600 m/s; and a deeper high-velocity material with Vs exceeding 1600 m/s. The maximum investigated depth was approximately 150 m. The subsurface structure exhibited lateral variability, particularly at greater depths. A comparison with seismic refraction results shows consistent velocity trends and similar near-surface layer depths, with both methods identifying comparable layering; however, SWI provides a more continuous and laterally detailed representation of velocity variation than the refraction model. This study demonstrates that the SWI is a reliable method for estimating near-surface Vs and provides crucial insights into subsurface stiffness variations.

Keywords: surface wave inversion (SWI), shear-wave velocity (Vs), multi-channel analysis of surface waves (MASW), near-surface geophysics, sesmic refraction, velocity modeling

1. INTRODUCTION

Surface waves are often treated as noise in conventional body-wave processing; however, their dispersive behavior makes them a highly useful tool for estimating near-surface shear-wave velocity (Vs). The physical basis is straightforward: in a vertically heterogeneous medium, different frequencies of Rayleigh waves propagate with different phase velocities because they sample different effective depths[1]. High frequencies are controlled by shallower materials, whereas lower frequencies record deeper structures. This frequency-dependent behavior provided the basis for inverting the dispersion curves into a Vs model.

The main advantage of Surface Wave Inversion (SWI) is its sensitivity to shear stiffness[2]. Compared to methods that primarily estimate compressional-wave properties, SWI provides direct access to the most relevant parameters for assessing rigidity, weathering contrasts, and near-surface mechanical variation. Therefore, surface-wave methods have become the standard for site characterization and shallow geophysical investigations[3]. Recent studies have expanded multi-channel analysis of surface wave (MASW) to a wide range of near-surface problems, including soil characterization[4], engineering site assessment[5], and joint inversion with other seismic methods[6]. The non-uniqueness of the inversion and the role of uncertainty have also received increasing attention[7,8]. However, surface-wave methods should not be treated as exact interface-mapping tools. SWI is inherently non-unique, with multiple models capable of fitting the same dispersion behavior[9], whereas the vertical resolution decreases with depth.

The southwestern Arabian Shield is a geologically complex crystalline basement terrain that has received limited attention in surface-wave literature. Further, an integrated SWI and seismic refraction workflow has not been applied to characterize the near-surface Vs structure of this region.

Therefore, in this study, we applied SWI to a real seismic line acquired in the Khamis Mushait area within the Abha region. Data were processed shot-by-shot using winMASW, with each shot treated as an independent one-dimensional (1D) inversion. The resulting Vs profiles were integrated in Surfer to construct a continuous pseudo-two dimensional (2D) Vs section. Overall, this study aimed to document the applied workflow, interpret the

Published under an exclusive license by KFUPM

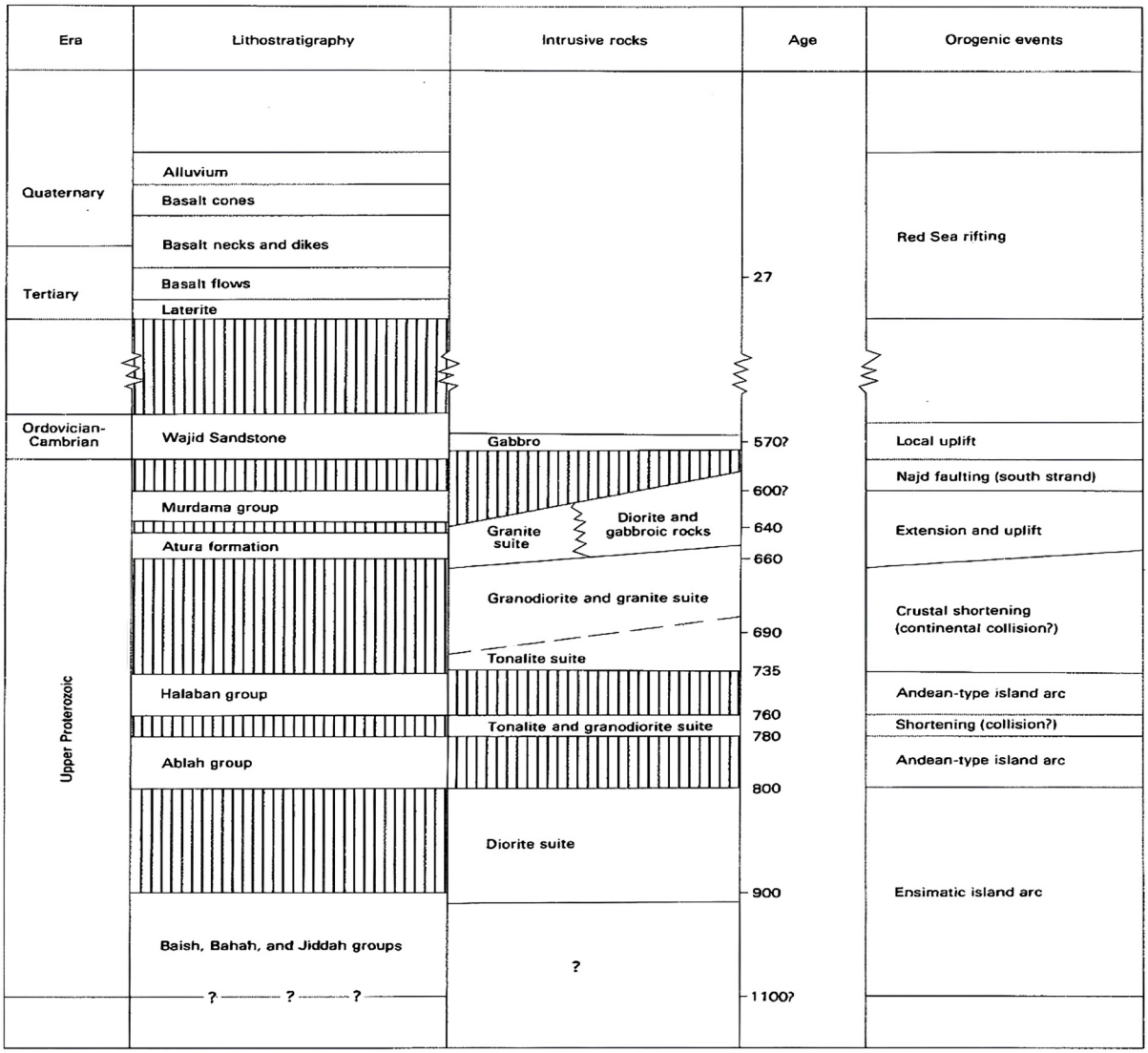

Figure 1. Stratigraphic and tectonic history of the Abha Quadrangle [10]

resulting subsurface velocity structure, compare it with independent seismic refraction results, and assess the key uncertainties that influence the reliability of the final model.

2. STUDY AREA

2.1. Geological Background. The Khamis Mushait area is situated near the center of the Abha Quadrangle within the southwestern Arabian Shield, a region characterized by a complex geological history involving multiple tectonic and magmatic phases [10]. The dominant lithological units are Late Precambrian, including the metavolcanic and volcanoclastic rocks of the Halaban Group and metasedimentary sequences of the Murdama Group (Figure 1). These units originally formed in an island arc setting and were subsequently modified by subduction-related tectonism and magmatism during the Neoproterozoic [10], contributing to the accretion of the Arabian Shield.

Following their formation, these sequences were intruded by a variety of plutonic bodies, including tonalite, granodiorite, granite, diorite, and gabbro, which were emplaced approximately 780–570 Ma [10]. This intrusive activity reflects the transition from arc-related magmatism to post-collisional tectonic regimes. This region has experienced significant crustal shortening, followed by extensional deformation and uplift. One of the most prominent structural features is the Najd Fault System, which is a major northwest-trending fault network that has strongly influenced the structural framework of the area and controlled the emplacement of younger dikes and fractures.

The study area around Khamis Mushait is structurally complex and contains a dense network of faults, dike swarms, and intrusive bodies (Figure 2). The area is predominantly underlain by granodioritic and tonalitic rocks with localized alluvial deposits and younger volcanic-related materials [10]. The presence of multiple fault strands and post-tectonic basaltic dikes indicates a prolonged and multistage deformational history. In addition, minor occurrences of younger sedimentary units, such as the Wajid Sandstone and Quaternary volcanic deposits, suggest that tectonic and magmatic processes, such as Red Sea rifting, continued into more recent geological periods.

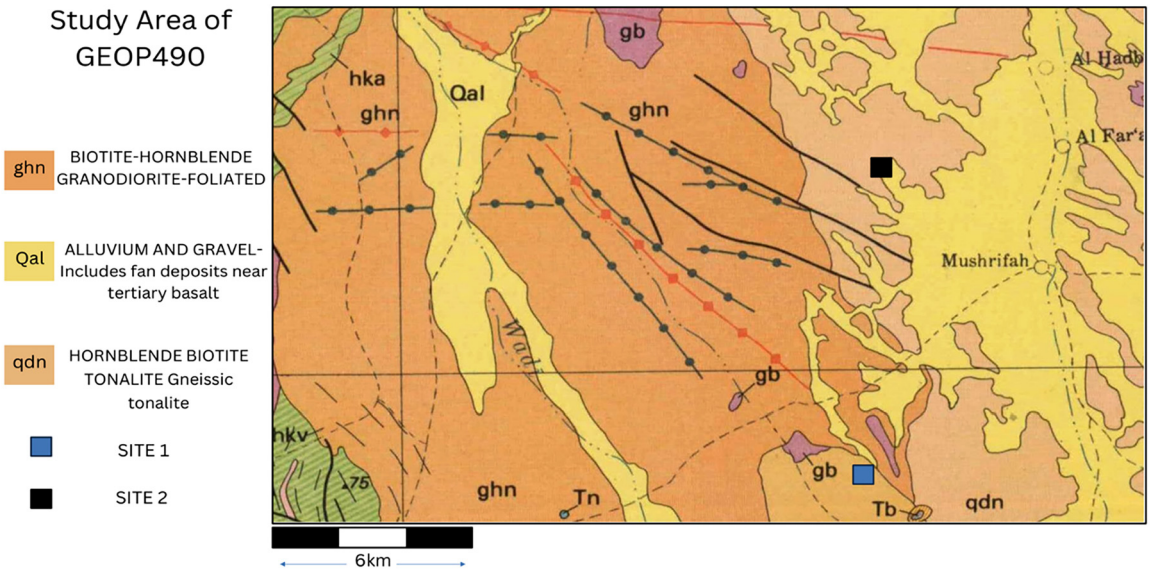

Figure 2. Geologic map of the Abha Quadrangle [10]

This geological complexity provides favorable conditions for subsurface investigations. Structural elements, including faults and dike contacts, are key targets because of their association with fractured zones and sharp property contrasts. Integrating geological mapping with geophysical methods improves the characterization of subsurface structures and enhances the interpretation of the crustal architecture in the study area.

2.2. Seismic Data Acquisition. Given the geological complexity of the study area, a seismic survey was conducted to investigate subsurface velocity variations. A seismic refraction survey was conducted during the GEOP 490 field camp in the Khamis Mushait area. The acquisition consisted of an 1840-m long profile with 231 geophones deployed at a uniform spacing of 8 m along the survey line. The geophone spread consisted of 121 single-and 110 three-component geophones arranged in an alternating pattern.

A weight-drop source was used to generate the seismic energy, providing a repeatable and controlled source suitable for near-surface investigations. In total, 185 shot points were acquired along the profile, with 16 stacks recorded at each shot location to improve the signal-to-noise ratio.

The relatively dense spatial sampling and long profile length provided sufficient coverage for both the refraction and surface-wave analyses. The short geophone spacing and large number of shots ensured adequate resolution of the surface-wave dispersion characteristics required for the subsequent surface-wave inversion processing.

3. METHODOLOGY

The SWI workflow consisted of four main stages: generation of a dispersion image for each shot gather, automatic extraction of the dominant dispersion curve using winMASW, inversion of the extracted curve to obtain a 1D Vs profile, and spatial interpolation of the resulting profiles in Surfer to produce a continuous pseudo-2D Vs section. This workflow reflects the standard practice in active-source surface-wave analysis and follows the processing structure implemented within winMASW, combined with grid-based post-processing for spatial visualization.

3.1. Dispersion Extraction. Each shot gather was processed independently. Prior to dispersion analysis, basic preprocessing steps were applied to improve data quality and ensure consistency. The first trace of each shot gather was removed to suppress near-offset source effects and improve the stability of the dispersion analysis. In addition, only the first 12 traces adjacent to the shot location were selected for dispersion analysis, corresponding to a maximum offset of 96 m. These near-offset traces contained the clearest and most coherent surface-wave energies, whereas traces at larger offsets exhibited reduced signal coherence owing to geometric spreading and source effects. A representative shot gather is shown in Figure 3. The data exhibit clear dispersive behavior, with Rayleigh-wave energy propagating across the receiver array and exhibiting increasing arrival times with the offset. The near-offset traces display higher amplitudes and more stable waveforms, supporting the selection of a limited number of traces for reliable dispersion analysis.

Following preprocessing, dispersion curves were extracted using an automatic picking algorithm implemented in winMASW. Rayleigh waves were analyzed using phase-velocity analysis, and the software identified the dominant energy ridge in the frequency-phase-velocity spectrum. The resulting dispersion curves extended to sufficiently low frequencies, supporting inversion to a depth of approximately 150 m, as reflected in the velocity spectrum in Figure 4, which is consistent with the cumulative depth of the best-fit model obtained for Shot 91 (Table 1). Traces beyond the 12th offset were excluded because they did not contribute additional low-frequency energy and introduced noise that degraded the quality of the dispersion image.

Figure 4 shows an observed velocity spectrum, wherein the dominant dispersion trend appears as a continuous high-energy ridge. This ridge represents the primary Rayleigh-wave mode and serves as the input for inversion. Automatic picking ensured consistent extraction of this trend across all shot gathers, while minimizing subjective interpretation.

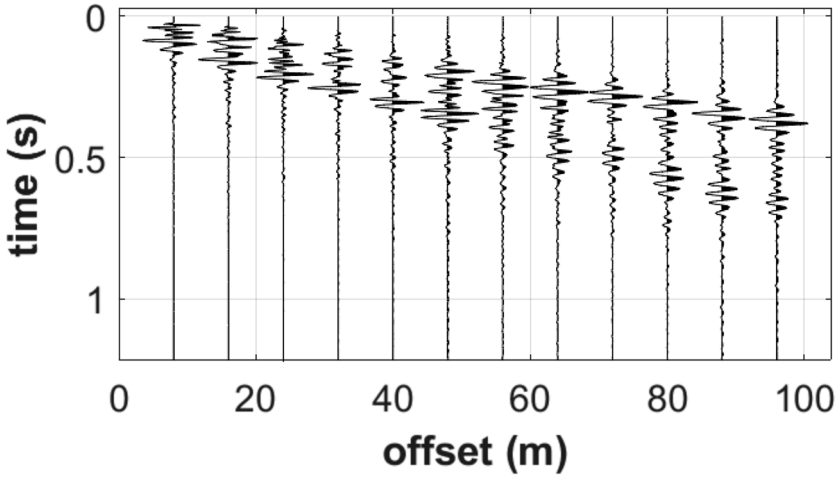

Figure 3. Shot gather for Shot 91, showing coherent dispersive Rayleigh-wave energy used for surface-wave analysis

3.2. Inversion Approach. The inversion was performed in winMASW on a shot-by-shot basis, with each shot being treated as an independent 1D problem. For each shot, the automatically extracted Rayleigh-wave phase–velocity dispersion curve was used as the input for the inversion. The objective was to determine a layered Vs model that reproduces the observed dispersion behavior in a physically consistent manner.

Inversion was performed using a genetic algorithm with 32 candidate models evaluated per generation over 60 iterations. Forward modeling was conducted using the ZVF configuration, which is consistent with the acquisition geometry and appropriate for Rayleigh-wave analysis. A total of eight modes were included in the forward calculation, which allowed the algorithm to account for potentially higher mode contributions.

The inversion output for each shot consisted of a layered model containing Vs, thickness, and cumulative depth. The representative best-fit model for Shot 91 is presented in Table 1. The model showed an overall Vs increase with depth, reflecting the expected transition from near-surface less-consolidated material to more competent subsurface layers.

The shallowest two to three layers exhibited very small thicknesses; in certain cases, this was on the order of a few tens of centimeters. These layers are not considered reliable for interpretation because the resolution of surface-wave methods at extremely shallow depths is limited and does not support centimeter-scale accuracy. Therefore, such layers are interpreted as numerical artifacts or over-resolved subdivisions introduced by the inversion process rather than as meaningful geological boundaries.

The interpretation focuses on the deeper portion of the model, where the layer thicknesses and velocity contrasts are more physically realistic and consistent with the resolving capability of the method. SWI is inherently nonlinear and non-unique; therefore, the derived Vs profiles represent the best-fit geophysical models rather than unique solutions. Despite this limitation, the inversion effectively captured the main variation in Vs with depth and provided a reliable basis for constructing the final pseudo-2D section.

3.3. Pseudo-2D Construction. Following the inversion, the set of 1D Vs profiles obtained from winMASW was spatially assembled using Surfer to generate a continuous pseudo-2D section along the seismic line. Each Vs profile corresponded to an individual shot location, and the final section was produced by interpolation between these discrete inversion points.

This step does not represent a true 2D inversion. Instead, the resulting section is an interpolation-based visualization constructed from independent 1D models. Interpolation was performed within Surfer using standard gridding techniques to convert the discrete Vs profiles into a continuous spatial distribution.

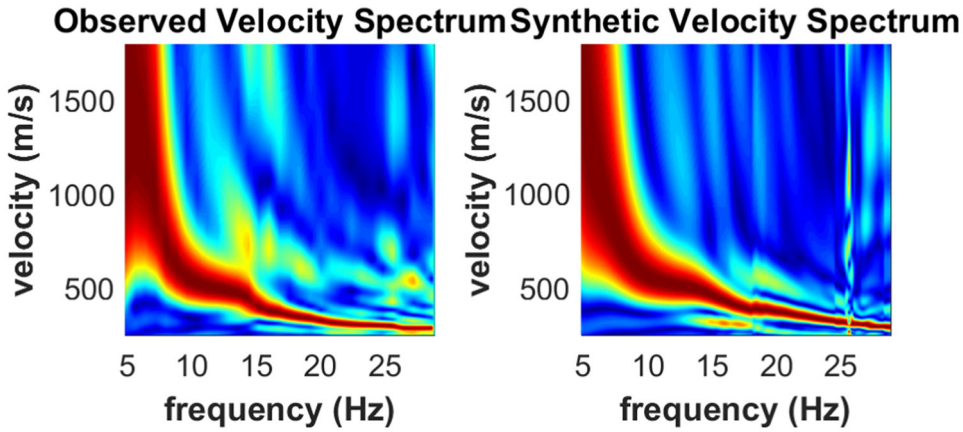

Figure 4. Observed (left) and modeled (right) velocity spectra for Shot 91, with good agreement between measured data and the inversion

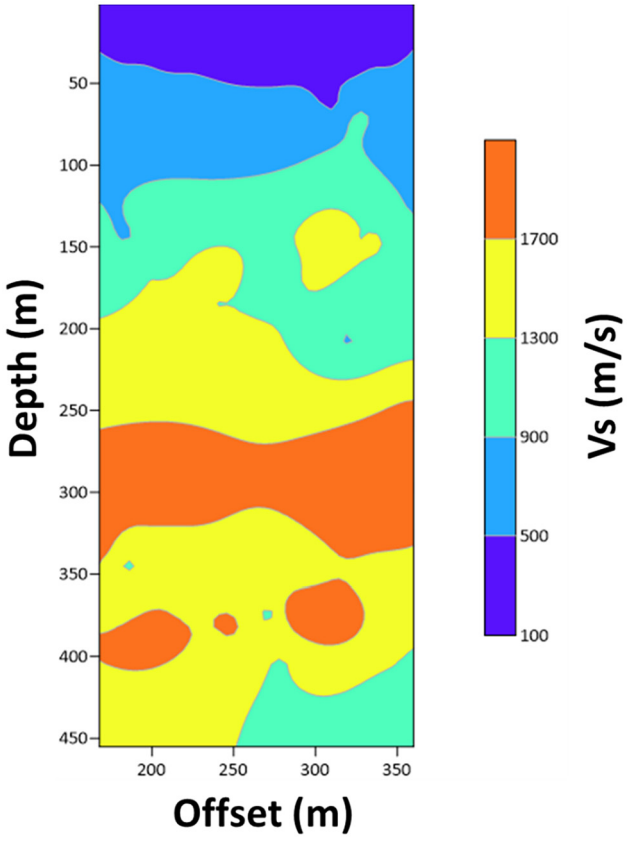

Figure 5. Intermediate pseudo-2D velocity (Vs) section (shots 21–45)

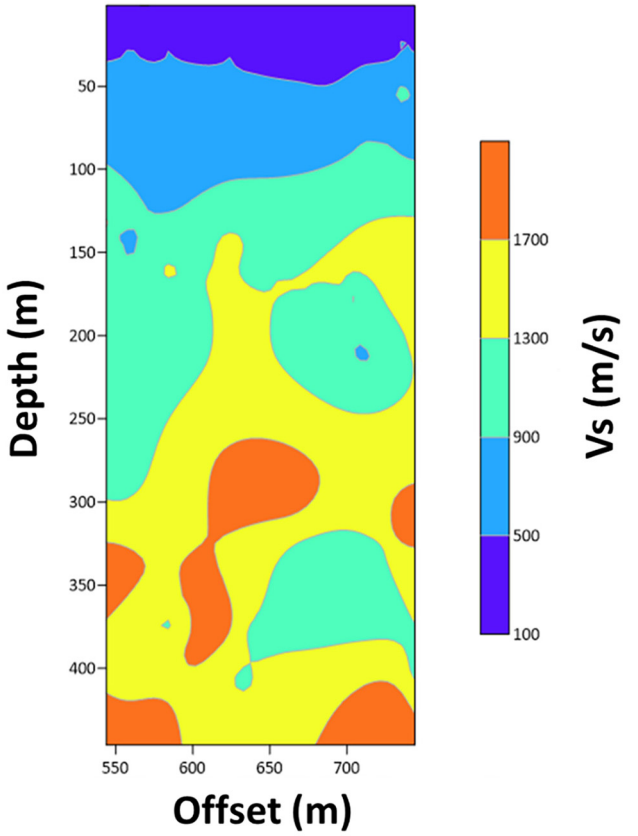

Figure 6. Intermediate pseudo-2D velocity (Vs) section (shots 70–95)

Intermediate pseudo-2D sections were generated at regular intervals (every 25 shots) to verify the consistency of both the inversion results and gridding process. These intermediate sections served as quality-control measures to ensure stability in the Vs profiles and continuity in the spatial interpolation. Examples of these intermediate sections are shown in Figures 5 and 6 and correspond to different shot intervals along the seismic profile. The output of this step is a pseudo-2D Vs section, which serves as the final processed dataset for subsequent analysis.

Table 1. *Best-fit one-dimensional velocity (Vs) model for Shot 91 from winMASW inversion*

Layer	Vs (m/s)	Thickness (m)	Depth (m)
1	100	0.2940	0.2940
2	155	0.5281	0.8221
3	179	0.8533	1.6753
4	308	1.8420	3.5173
5	358	5.5667	9.0840
6	292	6.6027	15.6867
7	237	8.0455	23.7321
8	471	10.5988	34.3310
9	792	38.8436	73.1746
10	1465	78.0157	151.1903
11	1202	176.4802	327.6705
12	3247	—	—

4. RESULTS AND DISCUSSION

4.1. Surface Wave Inversion Results. The final pseudo-2D Vs section obtained from the SWI is presented in Figure 7. This section shows a clear variation in Vs with depth, with an overall increase in velocity from the surface to depth.

The shallow part of the profile is dominated by low Vs values (blue), which were less than approximately 800 m/s. This zone extends to depths of approximately 80–120 m in the pseudo-2D model, although the deeper portion should be considered with caution. This low-velocity zone is laterally continuous along most of the profile, suggesting a uniform near-surface weathered layer across the survey line.

Below the low velocity layer, an intermediate velocity zone (yellow), with Vs values ranging from approximately 800–1600 m/s, occupies a large portion of the section. This layer was thicker and varied laterally. The transition from the low-velocity zone to this intermediate layer was gradual rather than sharp, indicating a progressive increase in stiffness with depth.

At greater depths (primarily below 250 m), high Vs values exceeding 1600 m/s (in red) appeared as irregular and discontinuous zones. These high-Vs regions were not laterally uniform, with noticeable variations in both depth and extent along the profile. In certain areas, these zones appeared at relatively shallow depths, whereas in others, they occurred deeper, suggesting variability in the deeper subsurface structure.

In Figure 7, Vs values are shown only to approximately 1600 m/s. The best-fit inversion model for Shot 91 (Table 1) included a Vs of 3247 m/s in its deepest layer. This value is unusually high

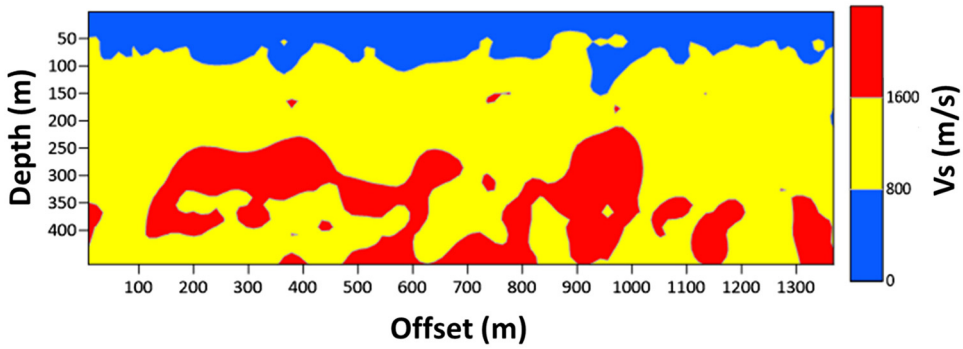

Figure 7. Final pseudo-2D velocity (Vs) section derived from Surface Wave Inversion (SWI)

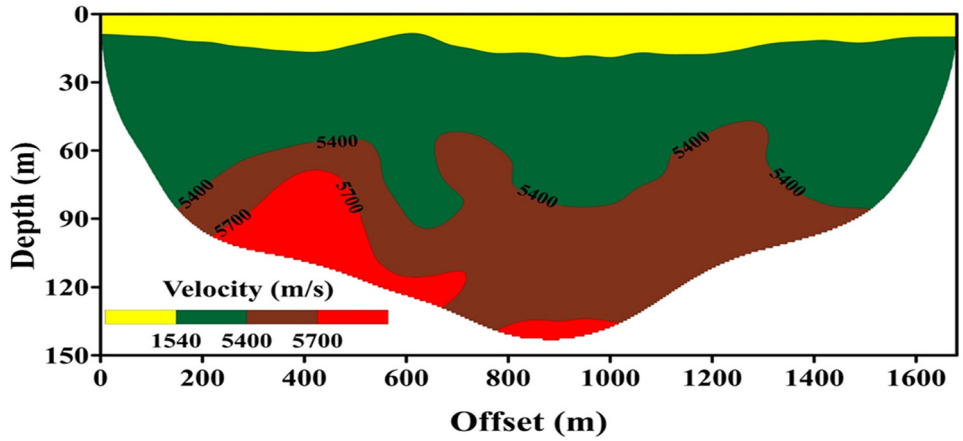

Figure 8. Seismic refraction velocity model along the same profile

for near-surface materials and is likely an artifact of the inversion rather than a geologically meaningful value. The deepest layer in the inversion model was poorly constrained because surface-wave sensitivity decreased significantly with depth, making the velocity of the lowermost layer unreliable. Therefore, this value should not be interpreted as a reliable estimate of the subsurface velocity and was excluded from the pseudo-2D visualization.

Overall, the SWI section indicated a layered subsurface characterized by a soft near-surface layer, transitional intermediate zone, and deeper, stiffer, or more competent material. However, the geometry of the deep high-velocity zones was not planar and exhibited significant lateral variability.

However, several sources of uncertainty affect the reliability of the pseudo-2D sections. First, surface-wave inversion is inherently non-unique; multiple Vs models can fit the same dispersion curve within the data noise level, and the genetic algorithm explores only a finite model space. Second, the use of only 12 traces per shot limits the maximum resolvable wavelength and, therefore, the maximum reliable depth of investigation. Third, the pseudo-2D section was constructed by interpolating independent 1D models and did not consider the lateral heterogeneity within each shot gather. The shallow layers, with thicknesses in centimeters, are considered numerical artifacts of the parameterization rather than resolved geological boundaries. Therefore, interpretation should focus on the main velocity zones rather than the fine-scale layer boundaries, particularly at depth.

4.2. Comparison with Seismic Refraction. A seismic refraction model (Figure 8) was used as an independent reference for comparison with the SWI-derived Vs section. Both results show a consistent overall trend of increasing velocity with depth, with a relatively low-velocity near-surface layer underlain by a higher-velocity material.

The near-surface layer identified in the refraction model corresponded to the low-Vs zone observed in the SWI section. Although the velocity values differ because of the different physical parameters involved (P-wave velocity (Vp) in refraction versus Vs in SWI), both methods indicate a low-velocity near-surface layer, with a transition to higher velocities occurring within a broadly comparable depth range along the profile. The refraction model suggests Vp ranges from 600 to 1200 m/s in this zone, which is broadly consistent with the low Vs values (below 800 m/s) derived from the SWI when considering typical Vp/Vs values for near-surface weathered materials. The depth to the first major velocity boundary agreed well between the two methods, both identifying the transition within a comparable depth range.

At greater depths, the refraction model exhibited a simplified and smoother velocity structure, whereas the SWI section displayed more gradual transitions and lateral variability. This difference reflects the fundamentally different sensitivities and resolution characteristics of the two methods rather than a contradiction between them.

Overall, the refraction results supported the main features observed in the SWI section, particularly the presence of a layered

structure and general increase in velocity with depth. The agreement between the two methods provided additional confidence in the reliability of the SWI results.

5. CONCLUSIONS

This study applied SWI to seismic data acquired in the Khamis Mushait area of southwestern Saudi Arabia to estimate the near-surface Vs structure. The workflow included dispersion extraction using winMASW, shotwise 1D inversion using a genetic algorithm, and spatial interpolation of the resulting profiles to construct a pseudo-2D Vs section extending to a depth of approximately 150 m.

The results revealed three main velocity zones: a low-velocity near-surface layer with Vs below 800 m/s, interpreted as weathered or less consolidated material; an intermediate transition zone with Vs ranging from approximately 800–1600 m/s showing lateral thickness variations along the profile; and deeper high-velocity material exceeding 1600 m/s, corresponding to a more competent bedrock. The deeper structures exhibit notable lateral variability, indicating that the subsurface is not laterally uniform across the survey lines.

A comparison with the seismic refraction results confirmed the overall layering pattern and general depth range of the near-surface low-velocity zone. Both methods identified a consistent trend of increasing velocity with depth, supporting the reliability of the SWI results. However, the SWI section provides more laterally continuous and detailed velocity variations than the refraction model, producing a smoother and more simplified structure.

The key limitations of this study include the non-uniqueness of the inversion process, the decreasing sensitivity of surface waves with depth, and the interpolation-based nature of the pseudo-2D construction. The lowermost inversion layer in several models produced unusually high Vs values that were considered inversion artifacts and were excluded from the interpretation. Thus, future research should consider the joint inversion of surface waves and refraction data and uncertainty analysis to better constrain the velocity model.

Overall, this study demonstrated that SWI is an effective and practical method for near-surface characterization of geologically complex crystalline terrain, providing valuable constraints on subsurface stiffness variations, with potential applications in site characterization and geotechnical assessment in the southwestern Arabian Shield.

AFFILIATIONS AND AUTHOR DETAILS

Undergraduate Author

Yazeed M. Alqahtani – *Department of Geosciences, King Fahd University of Petroleum & Minerals, Dhahran 31261, Saudi Arabia*; 0009-0001-2834-9891
Email: s202221940@kfupm.edu.sa

Corresponding Author

Sherif M. Hanafy – *Research Mentor, Associate Professor, Department of Geosciences, King Fahd University of Petroleum & Minerals, Dhahran 31261, Saudi Arabia*; 0000-0003-4568-2941
Email: sherif.mahmoud@kfupm.edu.sa

ACKNOWLEDGEMENTS

The authors would like to acknowledge GEOP 490 field camp team at King Fahd University of Petroleum and Minerals for their support during data acquisition and fieldwork.

REFERENCES

(1) Xia, J., Miller, R. D. & Park, C. B. Estimation of near-surface shear-wave velocity by inversion of Rayleigh waves. Geophysics 64, 691–700 (1999).

(2) Foti, S., Parolai, S., Albarello, D. & Picozzi, M. Application of surface-wave methods for seismic site characterization. Surveys in Geophysics 32, 777–825 (2011).

(3) Olafsdottir, E. A., Erlingsson, S. & Bessason, B. Open-source processing of surface wave data for shear-wave velocity profiling. Soil Dynamics and Earthquake Engineering 131, 106008 (2020).

(4) Park, C. B., Miller, R. D. & Xia, J. Multichannel analysis of surface waves. Geophysics 64, 800–808 (1999).

(5) Socco, L. V., Foti, S. & Boiero, D. Surface-wave analysis for building near-surface velocity models — Established approaches and new perspectives. Geophysics 75, 75A83–75A102 (2010).

(6) Tran, K. T. & Hiltunen, D. R. One-dimensional inversion of full waveforms using a genetic algorithm. Journal of Environmental & Engineering Geophysics 17, 197–213 (2012).

(7) Boiero, D. & Socco, L. V. Retrieving lateral variations from surface wave dispersion curves. Geophysical Prospecting 58, 977–996 (2010).

(8) Maraschini, M. & Foti, S. A Monte Carlo multimodal inversion of surface waves. Geophysical Journal International 182, 1557–1566 (2010).

(9) Ivanov, J., Miller, R. D. & Holliger, K. Multichannel analysis of surface waves (MASW): Theory, applications, and challenges. Geophysics 84, WD1–WD13 (2019).

(10) Greenwood, W. R. Geologic map of the Abha Quadrangle, Sheet 18F, Kingdom of Saudi Arabia. Saudi Arabian Deputy Ministry for Mineral Resources, Geologic Map GM-75 (1985).